



City Research Online

City, University of London Institutional Repository

Citation: Ioannou, E. & Sayma, A. I. (2017). Full Annulus Numerical Study of Hot Streaks Propagation in a Hydrogen-rich Syngas-Fired Heavy Duty Axial Turbine. Proceedings of the Institution of Mechanical Engineers, Part A: Journal of Power and Energy, 231(5), pp. 344-356. doi: 10.1177/0957650917706861

This is the accepted version of the paper.

This version of the publication may differ from the final published version.


Permanent repository link: <https://openaccess.city.ac.uk/id/eprint/17346/>

Link to published version: <https://doi.org/10.1177/0957650917706861>

Copyright: City Research Online aims to make research outputs of City, University of London available to a wider audience. Copyright and Moral Rights remain with the author(s) and/or copyright holders. URLs from City Research Online may be freely distributed and linked to.

Reuse: Copies of full items can be used for personal research or study, educational, or not-for-profit purposes without prior permission or charge. Provided that the authors, title and full bibliographic details are credited, a hyperlink and/or URL is given for the original metadata page and the content is not changed in any way.

Full Annulus Numerical Study of Hot Streaks Propagation in a Hydrogen-rich Syngas-Fired Heavy Duty Axial Turbine

Journal Title
XX(X):1–11
©The Author(s) 2016
Reprints and permission:
sagepub.co.uk/journalsPermissions.nav
DOI: 10.1177/ToBeAssigned
www.sagepub.com/


Eleni Ioannou and Abdulnaser I. Sayma

Abstract

This paper presents a study of the effect of fuel composition on hot streaks propagation in a high-pressure turbine using a full annulus unsteady CFD analysis of the first two stages. Hot streaks result from the inherent non-uniformities of temperature profiles at the exit of the combustion chamber. Variations in composition arise from current challenges requiring gas turbines to adapt to fuel variations driven by the need to reduce CO_2 emissions through the use of synthetic hydrogen rich fuels (Syngas) typically generated from the gasification of coal or solid waste. Syngas containing 80% hydrogen has been used in this study in a heavy duty gas turbine modified to accommodate the low calorific value fuel. Calculations were conducted on the baseline gas turbine originally designed for natural gas for the comparative study. Applying combustor representative hot streak profiles, analyses were performed for different hot streak distributions and locations. Analysis of results focused on the segregation of cold and hot fluid patterns and the effects of hot streaks on secondary flows and temperature re-distributions up to the second turbine stage. The hot flow pattern is affected by the fuel composition, resulting in more concentrated thermal wake shapes for syngas when compared to the reference natural gas fuel. In effect, the interaction with the secondary flow leads to more intense flow turning of the pressure side leg of the horseshoe vortex in the first rotor passage. The higher temperature levels in the case of syngas, in combination with the effect of the enhanced secondary flow, result in higher radial spread of the hot fluid that tends to migrate towards the blade hub and tip with the effects being obvious further downstream the first turbine stage.

Keywords

syngas, CFD, axial gas turbine, hot streaks, secondary flows

Introduction

During the last decade the development of gas turbines burning syngas to replace natural gas together with the development of Integrated Gasification Combined Cycle (IGCC) concepts, with built in pre-capture technology, has been considered as one of the most promising solutions for efficient and low- CO_2 power generation [Gadde \(2006\)](#). Generally, syngas differs from natural gas in terms of composition, physical properties and calorific value. Syngas composition also varies depending on the gasification process, composition of feedstock and the clean up process after the gasifier. With syngas usually being diluted with H_2O and N_2 , for stable combustion and NO_x control, the Low Heating Value (LHV) is lower than the LHV of natural gas [Oluyede \(2006\)](#). In effect, more syngas is required to be burnt in order to maintain the same power output, when compared to the natural gas fired gas turbine. The lower molecular weight of syngas in combination with the dilution process (always compared to natural gas), results in different composition of the combustor products characterised by higher water content and lower molecular weight.

The lower molecular weight leads to increased volume flow rate at the turbine inlet that consequently introduces the need of certain modifications of the existing gas turbine design, some of them were discussed by [Chiesa et al. \(2005\)](#). The variation in composition leads to a variation in thermodynamic properties that affect the enthalpy drop into

the turbine stages. The isentropic enthalpy drop is affected by the higher specific heat, C_p and the lower ratio of specific heats, γ as described by Equation 1.

$$\Delta h_{is} = C_p(T_{in} - T_{ex}) \quad (1)$$

Compared to natural gas, the hydrogen-rich syngas increases the enthalpy drop that can be evaluated through the expression on Equation 1 [Chiesa et al. \(2005\)](#). The syngas fuel expands to higher pressure and hence increased temperature is expected at the turbine exit. For a syngas turbine operating at firing temperatures similar to those of a natural gas fired turbine, the original turbine needs to be adjusted in order to operate at the increased pressure ratio. Another point to be considered is that apart from the variation in temperature drop, the change of γ , alters the axial velocity component as described by the definition of Mach number, Ma in Equation 2 and thus the velocity triangles in the turbine affecting the hot flow path.

$$Ma = C_x / \sqrt{\gamma RT} \quad (2)$$

Corresponding author:

Eleni Ioannou, School of Mathematics, Computer Science and Engineering, City University London EC1V 0HB London UK.

Email: Eleni.ioannou.2@city.ac.uk

where C_x is the absolute velocity in the axial direction, T is the static temperature and R the gas constant.

Further to the effects related to the composition of combustion products, the combustor exit profile contains temperature non-uniformities in both radial and circumferential directions. Those non-uniformities, known as hot streaks, can affect the development of secondary flow enhancing local heat transfer [Burlet and Dorney \(1997\)](#); [Ameri et al. \(2007\)](#) and increasing aerodynamic losses [Sharma et al. \(1992\)](#); [Chaluvadi et al. \(2003\)](#).

In natural gas fired gas turbines the dominant mechanism of the temperature redistribution into the stages has been widely investigated. Kerrebrock and Mikolajczak first described it for high-speed compressors [Kerrebrock and Mikolajczak \(1970\)](#) for the case of rotor wake/stator interaction in a compressor stage. They found that the temperature wakes passing through the stators are transported towards the Pressure Side (PS) of the stator passage. This happens as a result of the difference of the absolute velocity at the inlet of the rotor, due to the temperature difference, a phenomenon known as segregation effect for wakes and hot streaks. Based on Equation 2 the only variable for a hot streak entering the rotor frame is the increased temperature when compared to the neighbouring colder flow. Hence, a difference in absolute velocity arises that induces a slip velocity between the hot and cold fluid entering at the rotational frame. When switching to syngas fuel, an additional parameter is addressed due to the difference of γ from the products of combustion of natural gas. Knowledge of the temperature migration pattern in a turbine, which is the subject of discussion in this paper, becomes essential in order to maintain the high turbine performance - maintaining the same high Turbine Inlet Temperature (TIT) - avoiding at the same time the thermal loads.

Experimental and computational studies have been performed on the effects of hot streaks migration through axial turbines. Such studies were limited to the hot section of the first stage. Early experimental studies were performed by [Butler et al. \(1989\)](#) using a Large Scale Rotating Rig (LSRR) [Joslyn et al. \(1987\)](#). He carried out a number of hot streaks experiments in a large-scale low speed axial turbine to confirm the tendency of separation of hot and cold fluid when entering the rotational frame that leads to the preferential heating of rotor PS, with the hot fluid moving towards the PS of the rotor and the cold towards the Suction Side (SS). Butler's experimental results indicated no change to the streamline pattern in the stationary frame for uniform $P_{o,in}$ confirming the theory first described by [Munk and Prim \(1947\)](#) and [Lakshminarayana \(1975\)](#).

In addition to the segregation effect, some 3D effects were observed such as a spanwise migration of the flow, especially on the PS of the rotor. That effect was attributed to the increase in secondary flow due to temperature gradients. The impact on vorticity production due to temperature non-uniformities was early investigated analytically by [Lakshminarayana \(1975\)](#) and later computationally by [Hermanson and Thole \(2002\)](#) who showed that zero streamwise vorticity is produced through a turbine stator blade passage when stagnation temperature distortion is not accompanied by gradients in Mach number and stagnation

pressure. The results of Hermanson and Thole demonstrated the need to consider more realistic turbine inlet profiles in the simulations due to the effect of pressure gradient on the magnitude of secondary flows. Later studies also highlight the need of combustion representative data with regard to the propagation of hot streaks, considering a combination of temperature non-uniformities and engine-realistic velocity at the turbine inlet [Koupper \(2014\)](#); [Griffini et al. \(2016\)](#).

Later CFD simulations [Basol et al. \(2011\)](#); [Ong and Miller \(2012\)](#) confirmed the additional secondary flow production due to hot streaks and the impact of that on the spanwise migration of hot fluid on the PS and SS of rotor blade. However, those are general trends and are quite dependent on specific conditions in different turbines. The major effect of the enhanced secondary flow in rotor passage is the distortion of the hot streak profile on the rotor PS (significant or not, depending on the turbine and combustor design) and the compression of the hot flow streamlines on the rotor SS, the importance of which is highlighted in terms of performance and coolant effectiveness.

The present study has been conducted in conjunction with a European Commission funded project (H2-IGCC) [ETN \(2008\)](#) aiming at investigation the effect of burning Hydrogen rich syngas in a gas turbine within an IGCC power plant. The H2-IGCC project also aims to provide technical solutions for the next generation IGCC power plants at component and system levels. To enable the study on the gas turbine, a generic turbomachinery design based on combustion of natural gas has been used as a reference, and was modified to burn hydrogen-rich syngas. The preferred modification to deal with the increased fuel volumetric flow rate is the re-staggering the first turbine stator blades to allow higher swallowing capacity of the turbine and hence keep the cycle pressure ratio unaffected. The main objective of this paper is to provide a better understanding of the hot streaks migration patterns associated with the change in fuel composition. During this project it was not possible to obtain a complete hot streak profile for the syngas fuelled machine as measurements were only done on a single prototype burner in a test rig. Combustor prototype measurements conducted towards the end of the project did not provide detailed temperature profiles at the combustor exit. Hence, this study is confined to a known pattern of hot streaks from natural gas combustion that was used in the analysis for both natural gas and syngas gas turbines and thus the emphasis on the migration patterns within the turbine. Emphasis was on the simulation of combustor - representative hot streak shapes applying 24 non-identical hot streaks circumferentially aligned with the original stator position avoiding any scaling methods. It is envisaged that a better understanding of the hot gases flow pattern in a natural gas and modified syngas gas turbine will provide a better understanding of the complex nature of the hot gasses migration in a turbine contributing towards the development of efficient hydrogen-rich syngas fired gas turbines.

Numerical method

An in-house finite volume unsteady RANS compressible flow solver has been used for the numerical study presented here. It is based on the methodology described by [Sayma](#)

et al. (2000) and Sayma et al. (2000), which has been previously validated against experimental data for unsteady CFD simulations Vahdati et al. (2000). The flow equations are discretised using a second-order accurate implicit scheme for unsteady flow calculations with inner Jacobi iterations and an outer Newton iteration procedure is used where the time step is fixed throughout the solution domain. The selection of the optimum number of time step is based on the physics of the phenomenon under investigation.

For optimum spatial discretisation a 3D semi-structured mesh approach is used for turbomachinery blades providing geometric flexibility, Sbardella et al. (2000). The approach makes use of a structured body fitted grid near the blade and an unstructured grid occupying the interface between the structured one around the blades as shown in Figure 1. Mixing planes have been used for steady state computations using a single blade passage with repeated periodic boundaries. With the steady state solution as the initial condition the unsteady calculations are performed with sliding planes between bladerows. For the sliding planes the solution is updated at the interface at each time step by interpolating the variables in the stator computational domain to get the rotor fluxes and in the rotor domain to get the stator fluxes. In the present simulation the one-equation Spalart and Allmaras (1994) turbulence model was employed.

Turbine Geometry and Setup Configuration

This section describes the modelling of the turbine including the geometry, boundary conditions and cooling configuration. The baseline engine used for this study is a generic F-class gas turbine based on the SGT5-4000F as prepared for the H2-IGCC project investigations Cerri and Chennaoui (2013). Allowing the compressor to operate at the original design point and the TIT being the same as on the natural gas fired machine, the matching between the compressor and the turbine may be preserved by the opening of the first turbine bladerow. By restaggering the first stator and increasing the vane cross-sectional area a higher amount of mass flow rate is permitted to pass and the turbine will operate at different design point. The generic machine presented in the current study was modified by opening the first stator blades of the turbine by 0.22° . Regarding the turbine efficiency, a small reduction of about 0.2% was found compared to the original design that is related to the higher velocity losses as a result of the higher volume flow rate. That reduction is consequently reflected to the gas turbine efficiency that was found to be about 0.4% lower than the corresponding natural gas fired turbine. More details regarding the methodology, based on which the generic machine was designed, have been published by project partners for the cycle and 1D analysis Cerri and Chennaoui (2013), CFD analysis for the compressor Nucara and Sayma (2012) and turbine design Kluxen et al. (2014).

The gas turbine comprises a four-stage HP turbine; this study is focused on the first two stages consisting of 69/79 and 66/77 number of stator and rotor blades respectively. A common approach would be to assume periodic flow and model a single sector of each bladerow in order to reduce the model size and the required computational time. Due to

the lack of common integer factor between the number of stator and rotor blades, a scaling method should be applied by changing the solidity of one of the bladerows which would eventually affect the temperature distribution and the unsteady effects of the inlet temperature distortion would not be captured accurately Clark (2008); Mayorca (2010). For the current simulation this error was avoided by running full annulus multi - bladerow calculations.

For the stator-rotor interaction, unsteadiness is caused by the pitchwise blade-to-blade non-uniformities arising from the adjacent bladerow. When modelling an unsteady problem in turbomachinery the spatial length scale is usually the blade pitch while the time scale chosen is the blade passing period. With reference to the first stationary bladerow 80 physical time steps per rotor blade passing were chosen and 5520 time steps were needed for one full revolution of the rotor with a rotational speed of 3000 rpm. The total wall clock time was in the order of 8 days for the four-stage full annulus simulation performed in a parallel environment of 72 Intel Xeon cores of 1.95 GHz for a total computational mesh of 40 million points. In order to get confidence on the unsteady simulations a grid independence study as well as a comparison of the averaged CFD values against through flow model results have been presented by Ioannou (2015).

Boundary Conditions

At the turbine inlet, the stagnation pressure, stagnation temperature and the flow angle are specified, while the static pressure is applied at the turbine outlet. To account for the unsteady flow mechanisms related to the temperature non-uniformities the total pressure gradients are assumed to be zero at the turbine inlet and the stagnation pressure in the hot streak is the same as in the main flow. Averaged values of inlet and outlet of the four-stages turbine are presented in Table 1 with the inlet stagnation temperature corresponding to the average value after applying the hot streak profile.

Table 1. Turbine inlet-outlet area averaged values.

	NG	SG
$T_{o,in}$ [K]	1713	1713
$T_{o,out}$ [K]	810	877
$P_{o,in}$ [MPa]	1.74	1.74
$P_{o,out}$ [MPa]	0.109	0.112
m_{in} [kg/s]	524.3	516.8
m_{out} [kg/s]	653.4	647.3

Two parameters with major influence on the propagation of hot streaks are the maximum to the average inlet temperature ratio and the hot streak shape that depends on the combustor design and fuel choice. Ideal shapes have been widely used in the literature with identical circumferentially applied hot streaks; however, measured temperatures at the exit plane of combustors exhibit only approximately symmetric circumferential variations and non-identical hot streak shapes, with relatively cool regions at the hub and casing end walls Povey and Qureshi (2009).

For the current project, due to the lack of experimental data, the hot streak profile was calculated based on traverse data provided by industrial partners for one hot streak from a test rig. The hot streak shape was then randomly

adjusted for each one of the 24 hot streaks in order to impose variability of the peak temperature in both radial and circumferential directions and get a combustor representative temperature profile. For the simulation of the hot streak profile a percentage of distortion was applied on the top of the inlet stagnation temperature. In Figure 2 the stagnation temperature contour plot shows the 24 hot streaks at the turbine inlet. The radial location of the inlet peak temperature is between 22-40% span and the ratio of the maximum total temperature over the average at the centre of each hot streak is 1.12.

Syngas composition

The same temperature profiles and levels were used for both simulations of the natural gas and syngas machines due to the lack of experimental data, with a TIT equal to 1713 K. In order to maintain the same inlet stagnation temperature levels between the two fuels, density variations were adjusted for syngas using constant values of γ and R of 1.28 and 307.7 J/kg K, respectively. For the current hydrogen-rich syngas fuel composition, shown in Table 2, the values of γ and R were defined based on NASA-polynomials McBride et al. (1993) and were used to define the average turbine inlet conditions. For the current analysis a stage-wise constant specific heat ratio approach has been followed for both fuels, as detailed aerodynamic computations on few stages are not considered to be very sensitive to variable gas properties Mare (2008).

Table 2. Volumetric fuel composition.

Parameter	Compound	Value	
		NG	SG
Volume fraction [%]	H_2	0.00	85.82
	CO	0.00	1.17
	CO_2	0.00	4.03
	N_2	3.50	8.98
	CH_4	92.00	0.00
	C_3H_8	4.50	0.00
LHV [MJ/kg]		50.06	33.4
C_p [$Jkg^{-1}K^{-1}$]		1156.7	1406.6
Gamma [γ]		1.33	1.28
R [$Jkg^{-1}K^{-1}$]		287	307.7

Film Cooling

In the case of syngas the higher H_2O content is expected to change the heat transfer rate and to result in an increase in turbine metal temperature. A solution that has been suggested in order to avoid turbine blade overheating and maintain the same firing temperature is to increase the turbine coolant Kim et al. (2011). However, to avoid cross dependences between different parameters while investigating the effects of the fuel composition, a total coolant mass flow rate of 25% of the compressor's inlet mass flow rate, that corresponds to approximately 130 kg/s, was used in both cases (natural gas and syngas) Cerri and Chennaoui (2013) to cool the first three of the four turbine stages. The walls have been set as adiabatic while a distributed source term method was developed for the

modelling of the coolant flow. The method uses uniformly distributed source terms that mimic the behaviour of the cooling injectors. The source terms are applied at each bladerow as patches corresponding to the area of cooling holes Romocea et al. (2013).

Results and Discussion

Combined Effects of Hot Streaks and Fuel Composition on Secondary Flow - Contribution of Syngas Stator Wake

The expression describing the secondary vorticity in the turbine rotor (Equation 3) can be used in order to understand the various contributions to the development of secondary flow He (2003). In the rotational frame the density gradients (first term at the right hand side) and the radial gradients of the stator exit flow angle (second term at the right hand side) are the driving factors for determining the development of secondary flow according to Equation 3. However, local effects are not described by Equation 3, such as the horseshoe vortex that is generally formed due to the thickness of the blade near the leading edge.

$$\frac{W^2 R_n}{2\Omega} \frac{\partial \omega_s}{\partial s} = (C \sin \alpha - \Omega R) \frac{r}{2\rho} \frac{\partial \rho}{\partial R} + C \cos^3 \alpha \frac{\partial}{\partial R} (R \tan \alpha) \quad (3)$$

In case of hot streaks the effects on the shape of velocity triangles has already been mentioned. The hydrogen-rich syngas fuel also influences the velocity triangles at the exit of each bladerow when compared to natural gas fired gas turbine. The axial component of flow velocity ($C_x = \sqrt{\gamma R T M a}$) is affected by the fuel composition and the flow temperature, the latter being influenced by the decrease of γ and the geometric modification of the turbine, as the pressure drop is decreased due to the change of the throat area of the first bladerow, consequently increasing the turbine exit temperature. The counteracting effects may result in small or significant changes of the flow velocity depending on the flow conditions such as the syngas composition and the net impact of a higher flow velocity in the hot streak might be weakened or enhanced.

Along with the effect of syngas on the stator exit velocity distribution, the density gradient is added to the contribution of the secondary flow development. In the general case of inlet temperature distortions, the positive density gradients on the upper part of the hot streak entering the rotational frame will reinforce the second term in Equation 3 that is responsible for secondary flow generation due to the velocity flow turning. The reduced molar mass of syngas, that is 27.03 g/mol compared to 28.26 g/mol for natural gas, reduces the magnitude of the radial density gradients and alters the first term in Equation 3 and consequently affects the secondary flow development through the rotor passage.

An additional aspect that affects the rotor passage unsteady flow field is the transport of the upstream stator wakes. Based on the theory of the thermal wakes transportation as has been described by Kerrebrock and Mikolajczak (1970), the main feature of the theoretical profile at the vanes exit is a peak temperature near the stator PS followed by a plateau and a decrease near the SS,

as shown in Figure 3 (dotted line) where the theoretically predicted circumferential temperature profile was drawn against the CFD results. The magnitude of the temperature peak (hatched area) is increased due to the increased tangential Mach number and relative flow angle, with syngas resulting in higher stagnation temperature excess in the stator wake. The temperature excess in the wake near the PS times the thickness of the wake gives the energy flux impinging on the stator PS. This means that for syngas there is a higher concentration of high energy fluid near the PS and lower near the SS.

In order to investigate the effects of syngas on the propagation of the hot fluid, the circumferential stagnation temperature at the exit of first stator is shown in Figure 4 (a). The values are plotted at 30% span to coincide with the hot streak centre, with a zoom of one hot streak wake that corresponds to approximately three vane wakes. A closer view reveals a different pattern where the wakes that correspond to one hot streak in case of syngas seem to be more concentrated resulting in lower minima and higher maxima compared to the natural gas profile. This observation can be further explained in combination with Figures 4 (b)-(c) where the surface streamlines distribution is shown along with the instantaneous stagnation temperature contours for the hot fluid entering the rotor passage. The film coolant injection does not allow the observation of the hot streak on the blades surfaces. However; the characteristics of the PS and SS legs of the horseshoe vortex can be seen with the separation saddle point at their intersection for both natural gas (Figure 4 (b)) and syngas fuels (Figure 4 (c)).

Based on the segregation effect of the hot streak entering the rotational frame, the cold fluid in the upstream stator wake convects towards the SS of the rotor blade. In Figures 4 (b)-(c) the wake can be identified by the low temperature region which shows a more concentrated wake shape for syngas compared to natural gas. The stator wake interacts with the PS leg of the horseshoe vortex affecting the separation line. Hence, in the case of natural gas the flow tends to separate further downstream indicating a weaker PS vortex leg compared to syngas case. In effect, there is stronger deflection of the streamlines along the SS of the first rotor blade for syngas case compared to natural gas due to the PS leg of the horseshoe vortex with the streamlines moving higher on the meridional plane.

The streamlines close to the first rotor SS are shown in Figure 5 for a hot flow passage for natural gas (a), (c) and syngas case (b), (d). The streamlines close to the SS deflect towards the tip due to the higher flow turning of the PS leg of the horseshoe vortex as shown in Figure 4 (b). The radial flow transport is increased in the case of syngas with the flow accelerating and moving the separation line to a higher location along the span and towards the blade midspan. Another observation on the differences of the flow between the two cases is the flow deflection on the tip region of the rotor SS that is less pronounced for the syngas case (Figure 5 (a)) compared to natural gas (Figure 5 (b)). Due to the difference in fuel composition, the effect of the radial density gradient could be weaker in the upper part of the blade passage in the case of syngas. The differences on the wake shape and the consequent effect on the development of the secondary flow has been attributed to the fuel composition;

however, the small difference on the opening of the upstream stator passage between the two fuel configurations could also contribute to the resulting wake shape.

Hot Streak Propagation and Radial Migration Up to the Exit of the Second Turbine Stage

The variation of the flow velocity and the consequent effects on the secondary flows are expected to affect the radial migration of the hot streaks passing through the blade passage. Figure 6 shows the circumferentially averaged spanwise distribution of the axial flow velocity at the exit of each bladerow for the reference natural gas fuel and the hydrogen-rich syngas where the velocity profiles were extracted at the exit plane of the absolute frame of reference. The velocity increase in the syngas case can be observed between 5-95% span along each bladerow exit plane indicating the effect of the increased flow temperature under the same blade coolant conditions. The syngas case displays a more pronounced flow turning that is also slightly moved along the span compared to the natural gas case profile due to the effect of the secondary flow as discussed along with Figure 5. At the exit of the second stage, the radial spread of the hot fluid is higher for the syngas case compared to natural gas case which is more clearly shown in Figures 7-10 for two neighbouring hot streaks.

The stagnation temperature contours in Figures 7 and 8 show the propagation of two hot streaks through the first rotor passage and the alteration of hot streak shape under the influence of secondary flows for natural gas and syngas, respectively. The propagation of the hot fluid is shown for an instant in time after one full revolution for four axial locations, at the passage inlet, mid-chord and outlet. The radial migration of the hot streak for the case of syngas is higher with the hot fluid moving radially towards both the hub and tip as it propagated towards the exit of the rotor passage resulting in more stretched shape. In effect, the hub and tip areas should experience higher heat load in the syngas case considering also the increased temperature values of the syngas case compared to the natural gas case.

For syngas fuel, the 3D effects are obvious at the exit plane with the radial spread of the hot streaks resulting in two distinct peak temperature areas that propagate close to the rotor PS and one close to the midspan of rotor SS (segregation effect). Previous numerical studies have also related the hot streak radial migration to the rotor passage secondary flow. He et al. (2004) observed higher radial hot streak migration close to the hub where a stronger secondary flow due to a passage-vortex was more visible than that near the tip. Roback and Dring (1993) studied the effects of spanwise hot streak location on the radial migration into the rotor passage. For different injection locations in the radial direction the accumulation of hot streak towards both the rotor hub and tip has been observed. The formation of two distinct peak temperature areas at the outlet of first rotor as a result of the radial migration into the rotor passage has been also mentioned in the literature Dorney et al. (2000); Dorney and Burlet (2001) that is in agreement with observations in this study.

The effect is not dominant in the natural gas case (Figure 7) where the magnitude of the hot streaks is significantly

lower compared to natural gas and the radial migration is weaker. Moreover, the effects of the non-identical hot streak shapes are obvious at the exit plane of the first stage for both fuels. The hot streak area variations and the multiple circumferential injection locations resulted differences in the shape and magnitude of the hot streaks as they propagate throughout the stage. The circumferentially averaged temperature distribution at the exit of the first stage (Figure 6) confirms also that the two temperature peaks with the hot streak centre are located between 50-60% span (compared to the inlet 40-50% span).

In the second stator bladerow the thermal driven secondary flow that is induced by the stagnation temperature gradients follows the same mechanism as in the rotating frame. The absolute streamwise vorticity (ω_s) is developed along the streamlines into the stator passage in a similar way to those in the upstream rotor, as the additional component of vorticity that arises due to the rotation (Equation 3) is usually very small in axial turbines. In a multi-stage turbine, account should be taken also of the secondary vorticity produced upstream, meaning that the entry vorticity ($\omega_{n(0)}$) is present due to the secondary flow in the first rotor bladerow. In Figures 9-10 the stagnation temperature contours show the propagation of two hot streaks through the second stator passage where similar observations can be made as in the first rotor passage. The effects of syngas on the radial migration of the hot streaks as it propagates throughout the stage are more obvious with the hot streaks being attenuated in the natural gas case. At the outlet plane of the second stator passage ($x/l=4.2$) the syngas hot streak centre occupies larger area along the span with the PS of the stator remaining at higher temperature compared to the blade SS. The observations confirm the presence of high temperature gradients downstream the first turbine stage with a higher contribution on the spread of the hot fluid for the case of syngas fuel. Higher temperature levels are expected along the blade span with the tip region area being affected as the hot fluid tends to migrate towards the tip and hub. The outcome of the current analysis should be considered during the specification of coolant effectiveness of the turbine blades for the syngas - fired gas turbines.

In Figures 8-9 the stagnation temperature contours show the propagation of two hot streaks through the second stator passage where similar observations can be made. The effects of syngas are more obvious with the hot streaks being attenuated in natural gas case. At the outlet plane of the second stator passage ($x/l=4.2$) the syngas hot streak centre occupies larger area along the span with the PS of the stator remaining at higher temperature compared to the blade SS.

Conclusions

This paper presented a numerical study of the aerodynamic and thermal effects of hot streaks propagation and the interaction with the secondary flow field in the high pressure turbine of an industrial gas turbine engine with particular emphasis on the effects of fuel composition. One of the main aims was to investigate the effect of using hydrogen rich syngas fuel on the hot streak migration pattern compared to the usually used natural gas. Although modifications had to be made to the turbine geometry to accommodate the low

calorific value syngas, both simulations have been conducted with the same inlet boundary conditions and coolant flow scheme to enable better understanding of the fundamental changes.

The thermodynamic properties of hydrogen-rich syngas in combination with the increased swallowing capacity of the turbine lead to a lower pressure drop and increased temperature levels downstream of the combustor. It was found that the hot gas flow path exhibits differences compared to the reference natural gas fuel. The significant changes of the velocity deficit and consequently enhanced secondary flow lead to an upward shift of the hot streak centre along the first rotor blade span.

In addition, the effects of fuel composition on the thermal wakes exiting the first stationary frame have been observed. Interpretation of the wake profile at stator exit reveals a different wake shape for syngas which is more concentrated compared to natural gas as a result of differences in composition and hence in vane exit velocities. The main significance of the generated thermal wake pattern is its effects on secondary flows. The current combination of the geometry modification and fuel composition exhibited beneficial effects on the tip region in terms of secondary flow and more intense flow turning of the pressure side leg of the horseshoe vortex. In effect of the secondary flow the hot fluid spreads higher towards the blades tip and hub as it propagates up to the exit of the second stage, increasing the heat load on the hub and tip regions.

Finally, the analysis showed a dependency on the hot streak shapes as non-identical hot streaks were applied at the turbine inlet with consequent differences on the magnitude of the propagation, while the effective film coolant injection didn't allow the observation of the hot streak migration on the blades surfaces. A future study aims to investigate the effects of film coolant on the current design in order to understand the combined effects of film coolant injection and hot streaks propagation in a hydrogen-rich syngas turbine.

Acknowledgements

This work has been co-funded by the European Union's 7th Framework Programme for Research and Development and coordinated by the European Turbine Network (ETN) as part of the H2-IGCC project. The authors gratefully acknowledge the financial support, data and the valuable comments received by the project partners.

References

- Gadde S Wu J Gulati A McQuiggan G Koestlin B and Prade B (2006) *Syngas Capable Combustion Systems Development for Advanced Gas Turbines*, ASME Paper No. GT2006-90970.
- Oluyede E O (2006) *Fundamental Impact of Firing Syngas in Gas Turbines*, Electric Power Research Institute.
- Chiesa P Lozza G and Mazzocchi L (2005) *Using Hydrogen as Gas Turbine Fuel*, J. Eng. Gas Turb. Power, 127, pp. 73-80.
- Burlet K L G and Dorney D J (1997) *Influence of 3D Hot Streaks on Turbine Heat Transfer*, International Journal of Turbo and Jet Engines, 14, pp. 123-131.
- Ameri A A Rigby D L Steinthorsson E Heidmann J and Fabian J C (2007) *Unsteady Turbine Blade and Tip Heat Transfer Due to*

- Wake Passing, Technical Report NASA/TM-2007-214942, E-16116
- Sharma O P Pickett G F and Ni R H (1992) *Assessment of Unsteady Flows in Turbines*, J. Turbomach., 114, pp. 79-90.
- Chaluvadi V S P Kalfas A I Hodson H P Ohyama H and Watanabe E (2003) *Blade Row Interaction in a High-Pressure Steam Turbine*, J. Turbomach., 125, pp. 14-24.
- Kerrebrock J L and Mikolajczak A A (1970) *Intra-Stator Transport of Rotor Wakes and its Effect on Compressor Performance*, Journal of Engineering for Power, 92 (4), pp. 359-368.
- Butler T L Sharma O P Joslyn H D and Dring R P (1989) *Redistribution of an Inlet Temperature Distortion in an Axial Flow Turbine Stage*, Journal of Propulsion and Power, 5 (1), pp. 64-71.
- Joslyn H D Power G D Verdon J M Dring R and Blair M F (1987) *The Effects of Inlet Turbulence and Rotor Stator Interactions on the Aerodynamics and Heat Transfer of a Large-Scale Rotating Turbine Model*, Technical Report NASA, CR-4079.
- Munk M and Prim R (1947) *On the Multiplicity of Steady Gas Flows Having the Same Streamline Pattern*, Proceedings of the National Academy of Sciences of the United States of America, 33 (5), pp. 137-141.
- Lakshminarayana B (1975) *Effects of Inlet Temperature-Gradients on Turbomachinery Performance*, Journal of Engineering for Power, 97 (1), pp. 64-74.
- Hermanson K S and Thole K A (2002) *Effect of Nonuniform Inlet Conditions on Endwall Secondary Flows*, J. Turbomach., 124 (4), pp. 623-631.
- Koupper Ch Caciolli G Gicquel L Duchaine F Bonneau G Tarchi L Facchini B (2014) *Development of an Engine Representative Combustor Simulator Dedicated to Hot Streak Generation*, J. Turbomach., 136, pp. 111007-1-10.
- Griffini D Insinna M Salvadori S Martelli F (2016) *Clocking Effects of Inlet Nonuniformities in a Fully Cooled High-Pressure Vane: A Conjugate Heat Transfer Analysis*, J. Turbomach., 138, pp. 021006-1-11.
- Basol A M Jenny P Ibrahim M Kalfas A I and Abhari R S (2011) *Hot Streak Migration in a Turbine Stage: Integrated Design to Improve Aerothermal Performance*, J. Eng. Gas Turb. Power, 133, pp. 061901-1-10.
- Ong J and Miller R J (2012) *Hot Streak and Vane Coolant Migration in a Downstream Rotor*, J. Eng. Gas Turb. Power, 134 (43161), pp. 051002-0510012.
- ETN (2008) *Low Emission Gas Turbine Technology for Hydrogen-rich Syngas*, European Turbine Network, h2-igcc.eu.
- Sayma A I Vahdati M Sbardella L and Imregun M (2000) *Modelling of 3D Viscous Compressible Turbomachinery Flows Using Unstructured Hybrid Grids*, AIAA Journal, pp. 945-954.
- Sayma A I Vahdati M and Imregun M (2000) *An Integrated Nonlinear Approach for Turbomachinery Forced Response Prediction. Part I: Formulation*, Journal of Fluids and Structures, 14 (1), pp. 87-101.
- Vahdati M Sayma A I and Imregun M (2000) *An Integrated Nonlinear Approach for Turbomachinery Forced Response Prediction. Part II: Case Studies*, Journal of Fluids and Structures, 14, pp. 103-125.
- Sbardella L and Sayma A I and Imregun M (2000) *Semi-Structured Meshes for Axial Turbomachinery Blades*, International Journal for Numerical Methods in Fluids, 32 (5), pp. 569-584.
- Spalart P R and Allmaras S R (1994) *One-Equation Turbulence Model for Aerodynamic Flows*, Recherche aerospaciale, 1, pp. 5-21.
- Cerri G and Chennaoui L (2013) *General Method for the Development of Gas Turbine Based Plant Simulators: An IGCC Application*, ASME Paper No. GT2013-94040.
- Nucara P and Sayma A I (2012) *Effects of Using Hydrogen-Rich Syngas in Industrial Gas Turbines While Maintaining Fuel Flexibility on a Multistage Axial Compressor Design*, ASME Paper No. GT2012-69780, pp. 511-522.
- Kluxen R Honen H and Jeschke P (2014) *Gas Turbine Expander Design Modifications for H₂-Rich Syngas Application*, International Gas Turbine Conference, Brussels, Belgium, 14-15 October.
- Clark J P (2008) *Design Strategies to Mitigate Unsteady Forcing*, Air Force Research Lab., Wright-Patterson AFB.
- Mayorca M A (2010) *Effect of Scaling of Blade Row Sectors on the Prediction of Aerodynamic Forcing in a Highly Loaded Transonic Compressor Stage*, J. Turbomach., 133, pp. 021013-021023.
- Ioannou E (2015) *The Effects of Temperature Distortion on Aerodynamics and Low Engine Order Forced Response in Axial Turbines*, Doctoral thesis, City University London.
- Povey T and Qureshi I (2009) *Developments in Hot-Streak Simulators for Turbine Testing*, J. Turbomach., 131, pp. 031009-15.
- McBride B J Gordon S and Reno M A (1993) *Coefficients for Calculating Thermodynamic and Transport Properties of Individual Species*, NASA Technical Memorandum 4513.
- Mare L (2008) *Modelling of Variable Gas Properties and Compositions in Turbomachinery Flow Simulations*, ASME Paper No. GT2008-51085.
- Kim Y S Lee J J Kim T S and Sohn J L (2011) *Effects of Syngas Type on the Operation and Performance of a Gas Turbine in Integrated Gasification Combined Cycle*, Energy Conversion and Management, 52, pp. 2262-2271.
- Romocaa A A Elbaz A M R and Sayma I A (2013) *Application of a CFD Film Cooling Model to a High Pressure Multistage Axial Turbine Fueled with Hydrogen Rich Syngas*, International Conference of Fluid Dynamics, Alexandria, Egypt.
- He L (2003) *Unsteady Flow and Aeroelasticity in Handbook of Turbomachinery*, 2nd Ed., (ISBN 0-8247-0995-0), Marcel Dekker, Inc. New York, Chap. 5.
- He L Menshikova V and Haller B R (2004) *Influence of Hot Streak Circumferential Length-Scale in Transonic Turbine Stage*, ASME Paper No. GT2004-53370.
- Roback R J and Dring R P (1993) *Hot Streaks and Phantom Cooling in a Turbine Rotor Passage: Part I-Separate Effects*, J. Turbomach., 115, pp. 657-666.
- Dorney D J Sondak D L and Cizmas P G A (2000) *Effects of Hot Streak/Airfoil Ratio in a High-Subsonic Single-Stage Turbine*, International Journal of Turbo and Jet Engines, 17, pp. 119-131.
- Dorney D J and Burlet K L G (2001) *Effects of Hot Streak Shape on Rotor Heating in a High-Subsonic Single-Stage Turbine*, International Journal of Turbo and Jet Engines, 18, pp. 15-29.

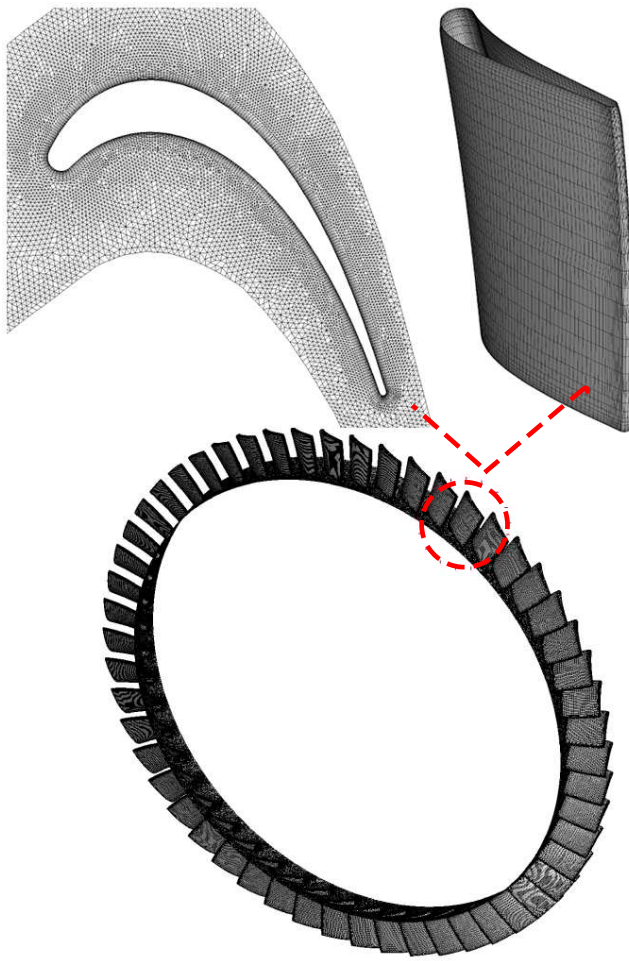


Figure 1. Computational grid for first rotor bladerow

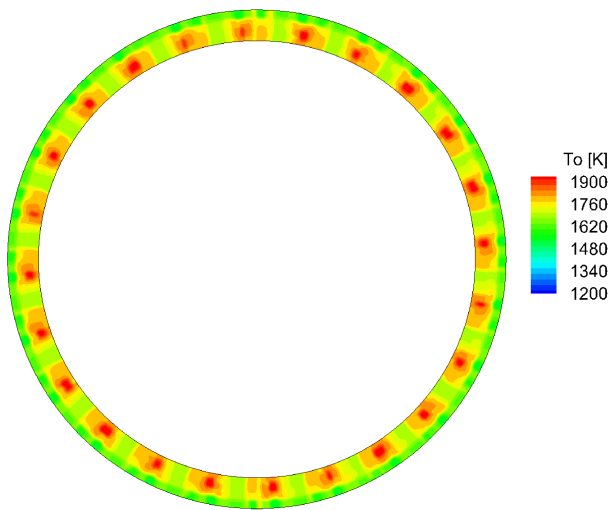


Figure 2. Stagnation temperature distribution at turbine inlet - 24 hot streaks

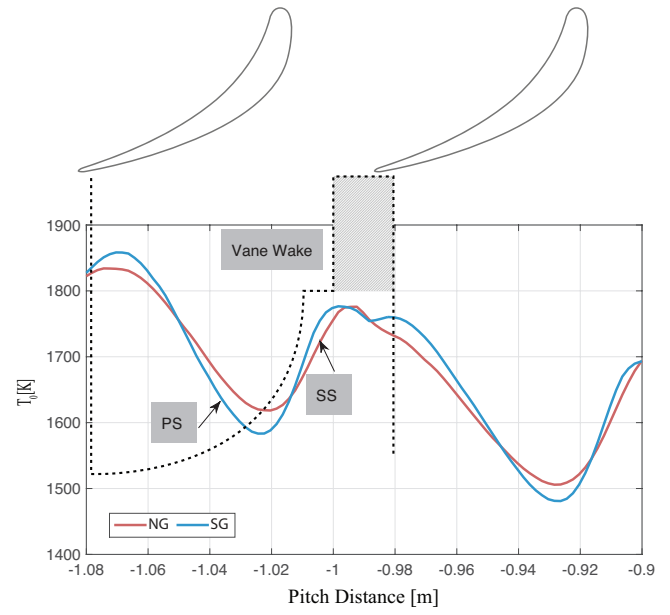


Figure 3. Circumferential stagnation temperature profile at $S1_{ex}$ at 35% with theoretically drawn circumferential profile (dotted lines)

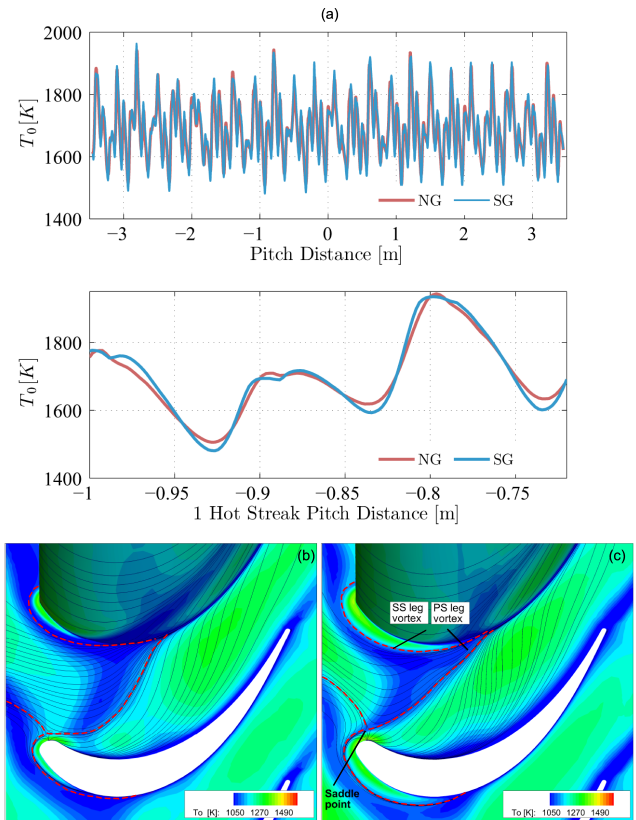


Figure 4. Circumferential stagnation temperature profile at $S1_{ex}$ at 35% with closer view of one hot streak vane wake (a) and horseshoe vortex system on R1 passage for natural gas (b) and syngas (c) cases

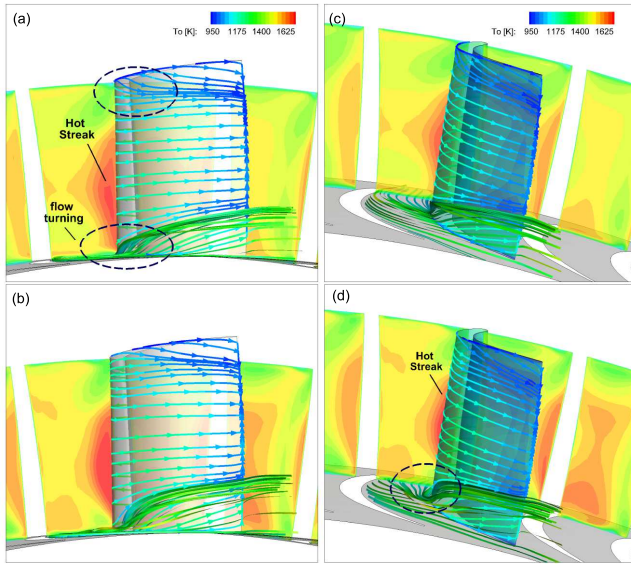
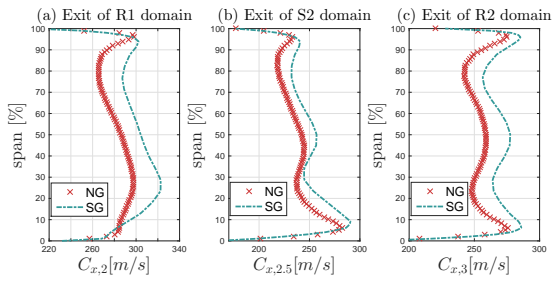
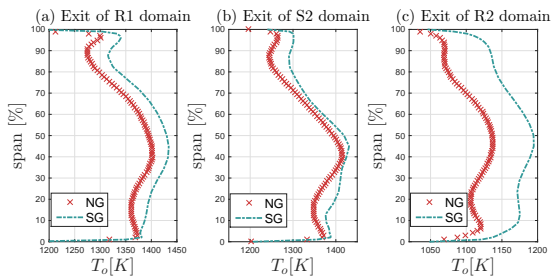


Figure 5. Stagnation temperature contours and streamlines close to $R1$ SS for natural gas case (a), (c) and syngas case (b), (d)



(a) Spanwise axial absolute velocity distribution at bladerows exit planes



(b) Spanwise stagnation temperature distribution at bladerows exit planes

Figure 6. Circumferentially averaged spanwise distribution at bladerows exit planes for natural gas and syngas

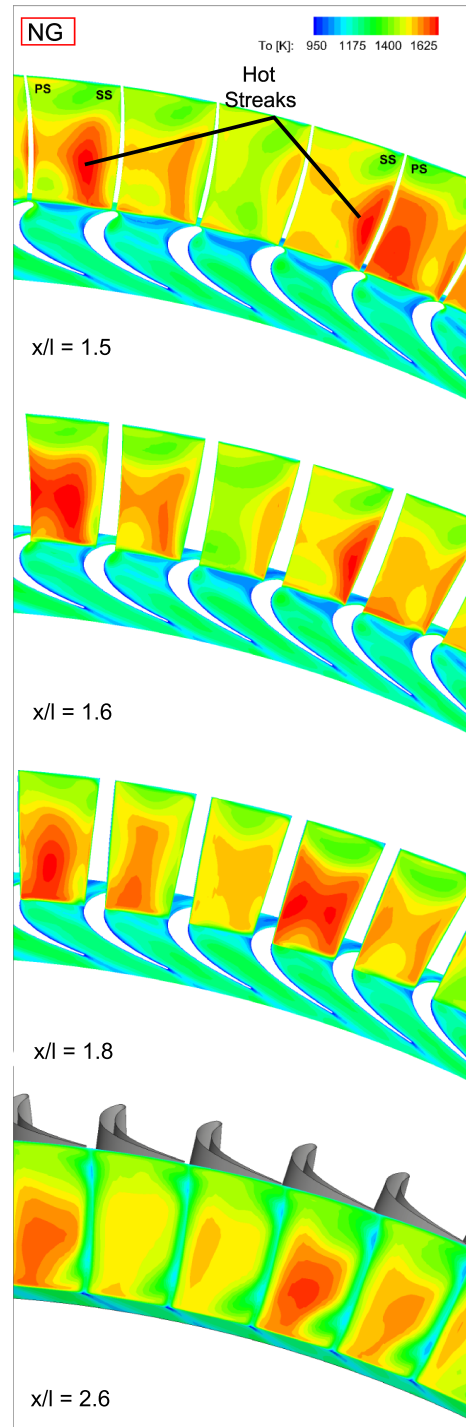


Figure 7. Stagnation temperature contours at $R1$ passage for natural gas

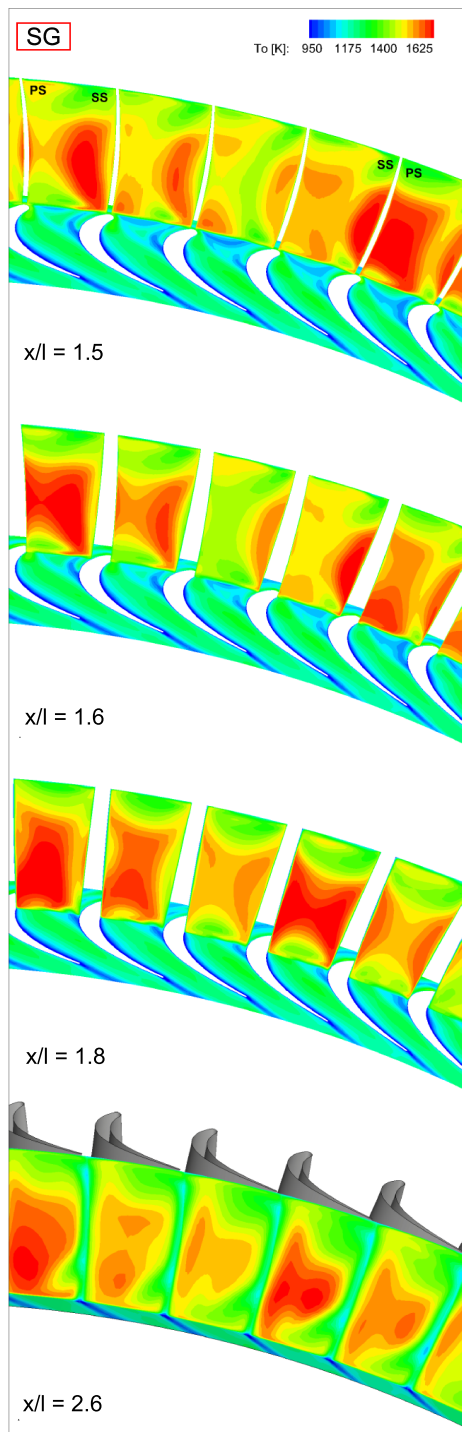


Figure 8. Stagnation temperature contours at $R1$ passage for syngas

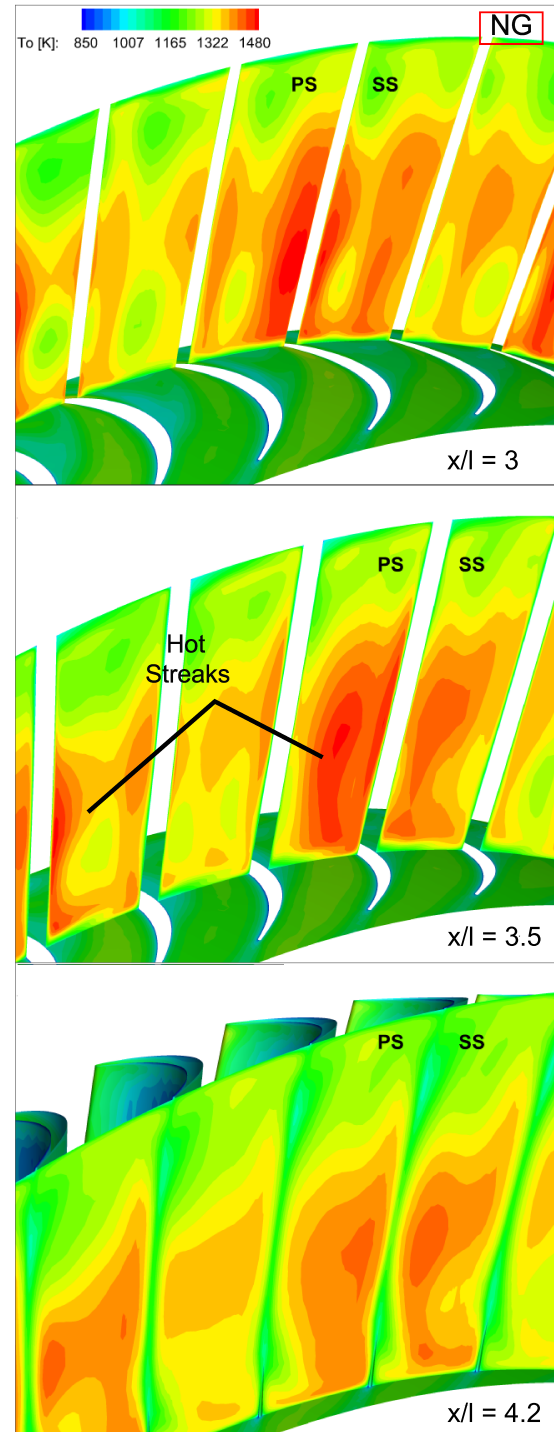


Figure 9. Stagnation temperature contours at $S2$ passage for natural gas

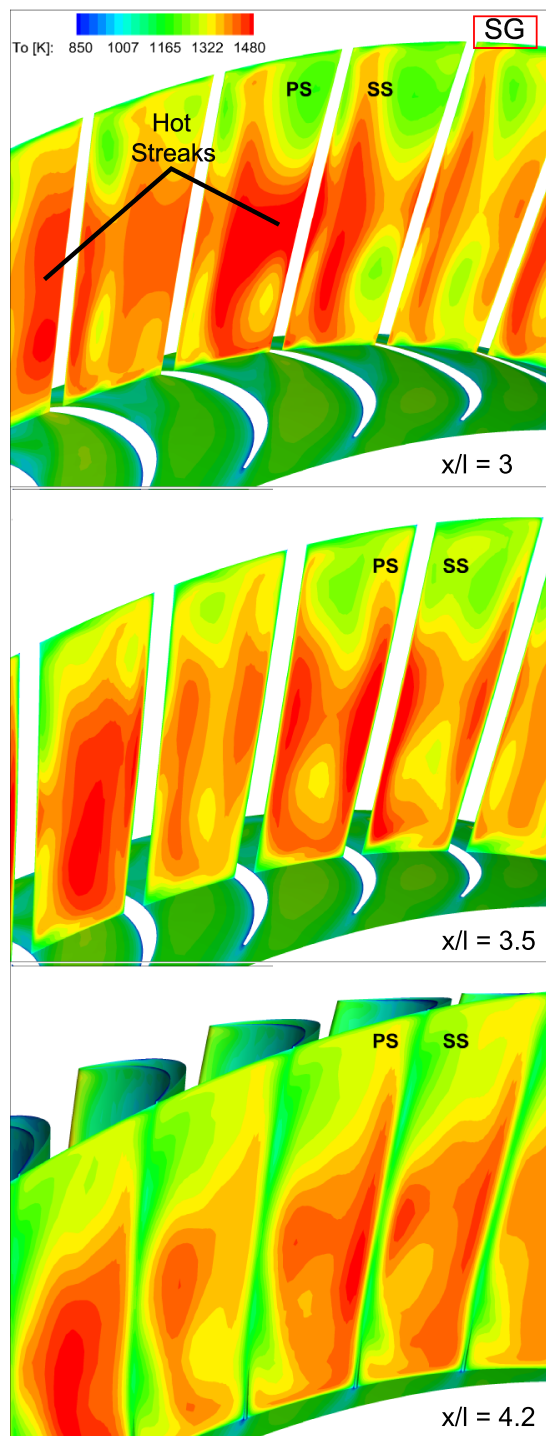


Figure 10. Stagnation temperature contours at $S2$ passage for syngas